1040-5488/06/8309-0666/0 VOL. 83, NO. 9, PP. 666–671
OPTOMETRY AND VISION SCIENCE

ORIGINAL ARTICLE

An Analytical Model Describing Aberrations in the Progression Corridor of Progressive Addition Lenses

RALF BLENDOWSKE, PhD, ELOY A. VILLEGAS, OD, and PABLO ARTAL, PhD

Laboratorio de Optica, Universidad de Murcia, Murcia, Spain

ABSTRACT

Purpose. In the progression corridor of a typical progressive addition lens (PAL) with an addition of 2.5 D, the power changes by roughly 1/8 D/mm. This renders a power difference of some 0.5 D across a typical pupil diameter of 4 mm. Contrary to this fact, PALs do work well in the progression zone. To explain why, we apply a simple model to derive wavefront characteristics in the progression zone and compare it with recent experimental data.

Methods. We consider a simple analytic function to describe the progression zone of a PAL, which has been introduced by Alvarez and other authors. They considered the power change and astigmatism, which are second-order wavefront aberrations. We include third-order aberrations and compare them with spatially resolved wavefront data from Hartmann-Shack-sensor measurements.

Results. The higher-order aberrations coma and trefoil are the dominant aberrations besides astigmatism as given by experimental data. According to our model, the third-order aberrations in the transition zone are strongly coupled to the power change and the cubic power of the pupil radius. Their overall contribution according to experimental data is nicely reproduced by our model. The numeric contribution of higher-order aberrations is small and, for practical purposes, the wavefront can be described locally by the second-order components of sphere and astigmatism only.

Conclusions. We propose a simple analytical model to understand the optics in the progression corridor and nearby zones of a PAL. Our model confirms that for typical pupil sizes, all higher-order aberrations, including the dominant modes of coma and trefoil, are small enough to render an undisturbed vision in the progression zone. Therefore, higher-order aberrations have a minimal impact on the optical performance of these lenses.

(Optom Vis Sci 2006;83:666–671)

Key Words: progressive addition lens, progression zone, Alvarez lens, higher-order aberrations, coma, trefoil, Hartmann-Shack-wavefront sensor

A presbyopic eye is lacking sufficient accommodation, that is, a variable increase of the lens power. Therefore, the presbyopic eye is not able to image close objects properly. Various optical tools exists to aid presbyopes, including diffractive contact and intraocular lenses, multizone refractive contact and intraocular lenses, accommodation intraocular lenses, and monovision. Most frequently, spectacle lenses are doing the job. Among them, bifocal glasses are still in use. They allow for only two different viewing distances, normally an object at infinity and one at a typical reading distance of some 400 mm. To this end, two lenses with two different powers are joined to form a compound lens, which is mounted as usual. Trifocal lenses extend this concept and increase the discrete numbers of sharply seen distances from two to three. Clearly, as a result of the depth of field, more or less extended regions are imaged sufficiently.

A progressive addition lens (PAL) offers the possibility to view at all distances in a continuous way. Additionally, the disturbing merging lines of a bi- or trifocal lens do not exist. The key concept of such a progressive addition lens is a so-called umbilicus or vertex line. Along that line, which might be straight or curved, the basic power change of the lens takes place. Objects at different distances can thus be imaged according to different positions on the vertex line.

The overall change in power needed to image both distant and near objects is called addition. It ranges from 0.75 D to 3.50 D, and a typical value is 2.50 D for a developed presbyope. The length

of the corridor where this power change happens to be might be some 20 mm. Clearly, this length is bounded by the size of the lens or more often by the lens mount. If we assume a linear power change along the vertex line, we expect a typical rate of power change given by some 1/8 D/mm. If we furthermore apply this number to a pupil diameter of 4 mm at the lens, we are led to a total power change of 0.50 D across the pupil. Therefore, one might wonder why a progressive addition lens works at all in the progression zone.

There is no principal obstacle to analyze existing PAL designs with commercial optical design software and to prove exactly that aberrations in the corridor are sufficiently small. However, the exact design data of PALs are proprietary and kept inhouse for obvious commercial reasons. Therefore, a simplifying approach, leaving detailed design concepts aside, might be helpful. Until now, this problem is dealt with only in a qualitative or, at best, semiquantitative way.[1]

For this reason, we consider a quite simple analytic model restricted to the progression zone of a PAL only. This kind of model has been extensively used in the (patent) literature.[2–5] We extend the exploitation of this model to the question of aberrations in the progression zone. The results obtained from this theoretical model are then compared with quite recent experimental data, which describe the wavefront characteristics of a PAL in a spatially resolved way.[6,7]

SIMPLE MODEL FOR THE PROGRESSION ZONE

To keep things fairly simple, we consider only the progressive surface of a lens. Because we are mainly interested in the aspect of local power change, the second surface of the lens can be neglected at least in the thin lens approach, because it will contribute only a spatially constant dioptric power. For convenience, we choose the first surface orientated toward the object as the progressive one, although today the second surface is increasingly used for this purpose. We are aware of the fact that for a proper and comprehensive description of the optics of a PAL, both surfaces, including the orientation of the lens relative to the eye, have to be taken into account.[1]

We consider a small part of the lens surface separating air from the lens material with refractive index n. The profile or elevation of the surface is described by the function $f(x,y)$ depending on Cartesian coordinates x and y. The wavefront change ΔW, that is the difference between the incoming and outgoing wavefront, according to the action of the surface, will approximately be given by

$$\Delta W(x,y) \approx (n-1)\cdot f(x,y) \tag{1}$$

The main assumption entering here is that the normal of the wavefront and the normal of the surface agree or include a small angle only.

We now determine the wavefront properties in more detail according to a simple model of the progressive zone of the PAL. The model is characterized by a constant rate of power change or, in other words, a linear increase of the power. This linear increase is restricted to the progression zone only. Any real lens will depart from this assumption to guarantee a smooth beginning and ending of the progression zone. We choose the coordinate system in such a way that the power increases along the positive y direction. The contour lines of constant values of the equivalent sphere, which simply are called power, are horizontal. Therefore, they are parallel to the x-axis. No prisms or specific recipe values are considered, which could be included additively in the model but are of no concern here. According to these assumptions, the surface sagitta is given by the following simple function[2–4]:

$$f(x,y) = \frac{a}{6}\left(y^3 + 3yx^2\right) \tag{2}$$

where a is some constant to be determined later. The second partial derivatives, which can be related to the surface power, are given by

$$\frac{\partial^2 f}{\partial x^2} = ay \qquad \frac{\partial^2 f}{\partial y^2} = ay \qquad \frac{\partial^2 f}{\partial x\,\partial y} = ax \tag{3}$$

We define the local power, or local equivalent sphere, by the following expression:

$$H = \frac{n-1}{2}\left(\frac{\partial^2 f}{\partial x^2} + \frac{\partial^2 f}{\partial y^2}\right) = (n-1)ay \tag{4}$$

The rate of power change is then given by the variation of H with the position y on the vertex line

$$\frac{\partial H}{\partial y} = a(n-1) = \overline{a} \tag{5}$$

where the constant $\overline{a} = (n-1)a$ determines the slope of the linear vertical increase in power, e.g., $\overline{a} = 1/8$ D/mm. Because the rate of power change does not depend on the x coordinate, only the vertical position y determines the power value at this point.

We now choose a point P_0 on the surface, which has the coordinates (x_0,y_0). The local neighborhood of the surface near P_0 could generally be described by a Taylor expansion of the surface in P_0. As a result of the simple analytic form of the surface elevation, equation 2, we can determine the properties of the surface and thus of the wavefront explicitly by

$$\begin{aligned}\Delta W(x_0+\tilde{x}, y_0+\tilde{y}) = \frac{\overline{a}}{6}\{&y_0^3 + 3y_0x_0^2 \\ &+ 6y_0x_0\cdot\tilde{x} + 3\left(y_0^2 + x_0^2\right)\cdot\tilde{y} \\ &+ 3y_0\cdot\left(\tilde{x}^2 + \tilde{y}^2\right) + 6x_0\cdot\tilde{x}\tilde{y} \\ &+ \tilde{y}^3 + 3\tilde{x}^2\tilde{y}\}\end{aligned} \tag{6}$$

where the distance from P_0 is measured by the variables $\tilde{x} = x - x_0$ and $\tilde{y} = y - y_0$. The optical interpretation of the various contributions is easy. The constant term (piston) is of no interest, because a general offset of the wavefront plays no role. The terms linear in the variable $\tilde{x}$ and $\tilde{y}$ represent a tilt of the wavefront and therefore a prismatic effect. Because we are not interested in this problem here, again, these terms are of no interest. The second-order terms are related to the power $\overline{a}\,y_0\cdot(\tilde{x}^2 + \tilde{y}^2)/2$, which changes along the meridian linearly with y_0 and to astigmatism $\overline{a}x_0\cdot\tilde{x}\tilde{y}$. Of special interest is the vertex line or the backbone of the progression corridor given by $x_0 = 0$. Here, obviously the astigmatism is zero. As described by the theorem of Minkwitz,[10] astigmatism increases laterally with the linear distance x_0 from the meridian. So far, this is all more or less well known.

The additional information stems from the remaining third-order terms:

$$W^{(3)} = \frac{\overline{a}}{6}\left(\tilde{y}^3 + 3\tilde{x}^2\tilde{y}\right) \tag{7}$$

which are independent of the position of P_0. They can be classified as coma and trefoil and can be related to the corresponding Zernike

coefficients by introducing the polar coordinates

$$\tilde{y} = \rho sin\theta \qquad \tilde{x} = \rho cos\theta \tag{8}$$

leading to

$$W^{(3)} = \frac{\bar{a}}{6}\rho^3\left(sin^3\theta + 3sin\theta cos^2\theta\right)$$

$$= \frac{\bar{a}}{12}\rho^3\left(sin3\theta + 3sin\theta\right) \tag{9}$$

Next, we rewrite the wavefront using normalized Zernike polynomials in which the double index scheme according to ANSI Z80.28 to 2004 is applied

$$Z_2^{-2} = \sqrt{6}\rho^2 \sin 2\theta \qquad Z_2^0 = \sqrt{3}\left(2\rho^2 - 1\right) \tag{10}$$

$$Z_3^{-3} = \sqrt{8}\rho^3 \sin 3\theta \qquad Z_3^{-1} = \sqrt{8}\left(3\rho^3 - 2\rho\right)\sin\theta \tag{11}$$

The normalized pupil radius is denoted by ρ. We rewrite the third-order contributions as

$$W^{(3)} = c_3^{-3}Z_3^{-3}(\rho, \theta) + c_3^{-1}Z_3^{-1}(\rho, \theta) \tag{12}$$

where

$$c_3^{-3} = c_3^{-1} = \frac{\bar{a}}{12\sqrt{8}}r_{max}^3 \tag{13}$$

and terms linear in ρ (tilt terms) are neglected. The semidiameter of the pupil is denoted by r_{max}. The result has the unit of microns if $\bar{a}$ is used with the unit diopter per millimeter and r_{max} is given in millimeters. It is worth mentioning that both coefficients are equal in this model. Because the surface is symmetric to the y axis, no contributions proportional to $cos\theta$ or $cos3\theta$ can appear. Therefore, the coefficients $c_3^3 = c_3^1$ do not contribute. This might be quite different in a real measurement, especially for curved vertex lines. We therefore combine the experimental contributions as follows:

$$c_{\text{trefoil}} = \sqrt{\left(c_3^3\right)^2 + \left(c_3^{-3}\right)^2} \qquad c_{\text{coma}} = \sqrt{\left(c_3^1\right)^2 + \left(c_3^{-1}\right)^2} \tag{14}$$

and compare c_{coma} and c_{trefoil} with the model predictions for c_3^{-1} and c_3^{-3}.*

For the sake of completeness, we give the second-order contributions according to the Zernike polynomials as well. The lateral astigmatism according to the Minkwitz theorem is given by

$$W^{\text{ast}} = \bar{a}x_0 \cdot \tilde{x}\tilde{y} = c_2^{-2}Z_2^{-2} \tag{15}$$

with

$$c_2^{-2} = \frac{1}{2\sqrt{6}}\,\bar{a}x_0\, r_{max}^2 \tag{16}$$

The defocus or power is related to

$$W^{\text{dfc}} = \frac{1}{2}\bar{a}y_0 \cdot \left(\tilde{x}^2 + \tilde{y}^2\right) = c_2^0 Z_2^0 \tag{17}$$

with

$$c_2^0 = \frac{\sqrt{3}}{12}\,\bar{a}y_0\, r_{max}^2 \tag{18}$$

*By personal communication with Charles Campbell (2006), the authors recently learned that Robert Webb noted (2003) that the Alvarez lens surface is the sum of equal amounts of coma, Z_3^{-1}, and trefoil, Z_3^{-3}, with a common coefficient, plus surface tilt, Z_1^{-1} d. These findings agree with our results but, unfortunately, they have not been published.

RESULTS

The experimental setup, basically a Hartmann-Shack wavefront sensor, has been described before.[6,7] Additional and explicit data are given to compare them with our model. All data are given for a pupil diameter of 4 mm. The PAL under test has a nominal addition of 2.00 D and a nominal sphere of 0.00 D in the far zone. The length of the corridor as given by the distance between the fitting cross and the center of the near verification circle is 18 mm. The grid of measurement positions is displayed in Figure 1, where we kept the original enumeration of the previous paper.[6] The distance between two measurement points in a column is 3 mm, which is the horizontal separation of the columns as well. Of main importance are the data along the vertex line. To illustrate the Minkwitz theorem, the lateral data at positions 2, 7, 11, and 17 are given as well.

In most commercial lenses, the rate of power change is clearly not linear. Therefore, we can expect a shorter effective length of the progression zone than the given 18 mm. The nonlinear effect can be seen clearly from the entries for the power rate $\bar{a}$ in which the maximum is reached before half of the length of the corridor (see Table 1). According to this reasoning, we fix the only parameter in our model to the mean value calculated from the data in the corridor as given in Table 1.

$$\bar{a} = 0.12 \text{ D/mm} \tag{19}$$

corresponding to an addition of 2.00 D and effective corridor length of 16.7 mm. We exclude the entries for zone 1 and 19 from further consideration, because they are located almost outside the progression zone.

As the next step, we discuss the wavefront profile across the pupil as predicted by the model. We chose a quite arbitrary pupil position, which is centered at y = 16 mm (see Fig. 2). The whole abscissa, as displayed in Figure 2, represents a pupil diameter of 4 mm. The curvature change of some 0.5 D along this distance is barely visible from the plot showing the demands to fabricate such a surface. For a given pupil position, a sphere fitted to this wavefront profile represents the defocus at this position. According to the small pupil size compared with the considered defocus, the

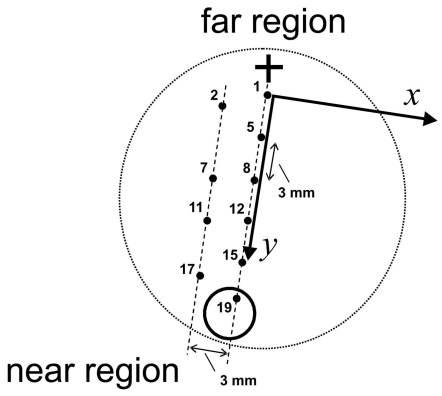

FIGURE 1.
Geometry of the measurement points and the applied coordinate system. The numbering scheme is the same as in reference 6. The distance between two points along the y axis is 3 mm. The two parallel lines have a distance of 3 mm as well. Points 1, 2, and 19, located near the fitting cross and close to the near verification circle, are already outside the progression zone.

TABLE 1.
Zernike coefficients for defocus converted to diopters in the third column; for a distance of 3 mm between the measurement points, the local power rate is calculated in the last column; the arithmetic mean value is used to evaluate our model

Zone Number	Defocus c_2^0 (μm)	Sphere D	Power Rate $\bar{a}$ D/mm
1 (far)	0.0810	0.1403	
			0.1256
5	0.2986	0.5172	
			0.1160
8	0.5000	0.8660	
			0.1755
12	0.8039	1.3924	
			0.0982
15	0.9740	1.6870	
			0.0905
19 (near)	1.1307	1.9584	
			$\bar{a}_{\text{mean}}$ =0.12

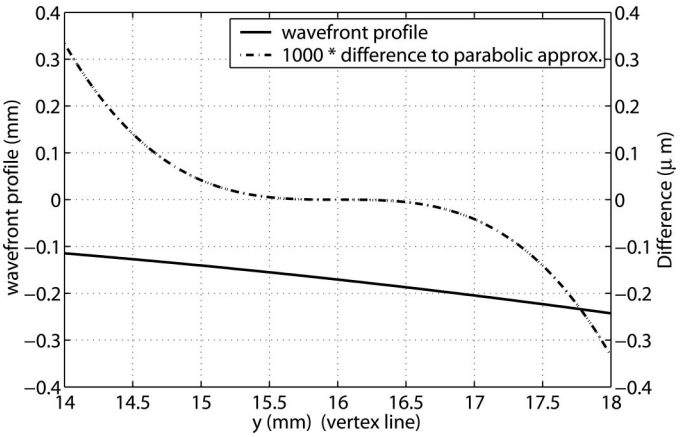

FIGURE 2.
The wavefront profile along the vertex line as described by our simple model is given by the solid line. At the position of 1 millimeter, a parabola is fitted to this wavefront profile. The difference between the parabola and the actual profile is a measure of higher-order aberrations. Pay attention to the scaled axis at the right side, which gives figures in micrometers.

sphere can safely be approximated by a parabola, which is related to the second-order wavefront aberration of defocus. This defocus determines the local addition, which a presbyopic eye will encounter at this position.

The difference between the actual wavefront and the parabola represents the higher-order aberrations. As Figure 2 shows for the parameter $\bar{a} = 0.12$ D/mm, the contribution of these aberrations in the plotted meridian is quite negligible. Although the difference spans a region of some 0.7μm, peak to valley, which is yet quite small, a further reduction occurs if the tilt of the wavefront is subtracted as well, leading to even smaller contributions.

The given reasoning is yet restricted to one meridian only and the whole pupil area has to be considered. To this end, we characterize the aberrations according to their Zernike coefficients as defined by equation 13. Again, for $\bar{a} = 0.12$ D/mm and a pupil diameter of 4 mm, we arrive at

$$c_3^{-3} = c_3^3 = 0.0283\ \mu\text{m} \tag{20}$$

This figure is proportional to $\bar{a}$ and it scales with the third power of the pupil diameter. For a lateral position of $x_0 = 3$ mm and again a pupil diameter of 4 mm, the astigmatism is given by

$$c_2^{-2} = 0.294\ \mu\text{m} \tag{21}$$

In comparison, both values resemble roughly a factor 10 between them. In other words, the astigmatism appearing lateral in a distance of 3 mm has a 10 times larger Zernike coefficient than the third-order aberrations exactly in the progression zone.

If we compare these predictions with the experimental data (see Table 2), we find a good correspondence concerning the following aspects. First, the experimental third-order contributions are nearly constant regarding spatial variation. Second, the ratio of coma and trefoil is roughly 1, as predicted by equation 13. Third, the absolute value deviates on average by not more than 14% for trefoil and 3.5% for coma.

Obviously, the agreement in absolute value might have been a result of the fit of the parameter $\bar{a}$. However, comparing the astigmatism, which takes place in the lateral direction, with the model prediction shows good agreement as well (see Table 3). This confirms the numeric value of $\bar{a}$ in an independent way. Again, the entry for zone 2 has to be omitted, because it is not located inside the transition zone.

To put it clearly, we do not claim a perfect match between the model data and the experimental results but an overall agreement only. Therefore, we do not go into further details of experimental uncertainties related to the exact position of the progression corridor, the inclination of the lens, or measurement errors of the Hartmann-Shack sensor.

To finish, we estimate the impact of the higher-order aberra-

TABLE 2.
Comparison of third-order Zernike coefficients with the model prediction for Insert Equation D/mm

Zone Number	Coma $\sqrt{(c_3^3)^2+(c_3^{-3})^2}$($\mu$m)	Trefoil $\sqrt{(c_3^1)^2+(c_3^{-1})^2}$ (μm)	Model $c_6 = c_7$ (μm)
1 (far zone)	0.0164	0.0099	
5	0.0285	0.0275	0.0283
8	0.0295	0.0374	0.0283
12	0.0280	0.0313	0.0283
15	0.0307	0.0251	0.0283
19 (near zone)	0.0095	0.0152	

TABLE 3.
Comparison of second-order Zernike coefficients for astigmatism with the model prediction for Insert Equation D/mm and a lateral distance of 3 mm

Zone Number	Astigmatism $\sqrt{(c_2^{-2})^2+(c_2^2)^2}$ (μm)	Model c_2^{-2}(μm)
2 (far)	0.141	
7	0.303	0.294
11	0.310	0.294
17	0.279	0.294

tions on visual acuity. For the sake of simplicity, we use the Strehl ratio as a measure. We are aware of the fact that the Strehl ratio does not relate directly to visual acuity, in particular for severely deteriorated images with a low quality.[8] However, it should be sufficient to estimate the influence of the aberrations under investigation. A convenient approach to calculate the Strehl ratio *SR* is the following approximation[11]:

$$SR \approx \exp\left[-\left(\frac{2\pi}{\lambda}\right)^2 \mathrm{rms}^2\right] \qquad (22)$$

which relates the squared RMS value of the wavefront deformation to the Strehl ratio. A first-order Taylor expansion reveals the more frequent formula. We recall that the squared RMS value of the wavefront deformation is simply given by the sum of the squared coefficients of the Zernike polynomials. In case of the coma and trefoil contribution, this results in a simple factor of 2 leading to

$$\mathrm{rms} = \frac{\overline{a}}{24} r_{max}^3 \qquad \text{(Coma, Trefoil)} \qquad (23)$$

where the result is in microns if $\overline{a}$ is used with the unit diopters per millimeter and r_{max} is given in millimeters. Assuming a wavelength of $\lambda = 0.55\mu$m, the Strehl ratio is given by

$$SR = 0.81 \qquad (24)$$

which usually is classified as diffraction-limited. Even for a 6 mm pupil diameter, the Strehl ratio has still a value of $SR = 0.$ Clearly, there will be no significant loss of visual acuity because of coma and trefoil.

Experimentally, we found that all other aberrations are at least one magnitude of order less than the dominant coma and trefoil. Therefore, their impact on visual acuity can be neglected and we can safely conclude that all higher-order aberrations, including coma and trefoil, have no impact on the visual acuity in the progression corridor.

These visual performance predictions agree with previous experimental work[9] in which the visual acuity measurements of the eyes looking through the corridor zones of the progressive lens were similar to those of the naked eye.

DISCUSSION

The design of a PAL, according to the second-order (or paraxial) properties of wavefronts, is mainly determined by the backbone of the lens, which is the vertex line, usually made up of nearly umbilic points. According to the theorem of Minkwitz, the second-order astigmatism is determined in the close neighborhood of the vertex line. Together with the rate of the power change, the second-order features of the transition region are fixed. By exploiting a simple model based on a cubic polynomial, which describes the surface in the transition region, we have derived some features of the third-order aberrations, including the following results. Coma and trefoil contributions are spatially constant in the transition region, they are of equal size, and are directly related to the rate of power change. The absolute values are quite small and should have no effect on visual acuity. Therefore, higher-order aberrations have a minimal impact on the optical performance of these lenses.

However, the final image quality at the retina depends on the complete optical system consisting of two elements: eye and PAL. In fact, the coupling of the aberrations of both elements could produce small changes of visual acuity as described by Villegas and Artal.[9]

In passing, it is worth mentioning that speaking of a 0.5-D difference in power across the total pupil, as we did in the introduction, is not totally meaningless. However, such a number is not able to cover the fact, that the parabola fitted to the wavefront across the whole pupil region is very close to the actual wavefront. The remaining differences are easily understood and negligible. Therefore, care should be taken to apply paraxial optics properties in a too simple way to predict nonparaxial behavior.

Our approach is clearly restricted to third-order contributions to wavefront aberrations by construction of the surface polynomial. This restriction, however, is not a very serious one because the experimental data do not show any relevant contributions for higher-order aberrations. This might change a bit for PALs with a very short and harsh progression zone as found in PALs for very small spectacle frames.

Our proposed simple model is restricted to the transition region and close to the vertex line. It is not able to predict anything for other regions of a PAL. However, the main feature of a PAL, besides cosmetic effects, is the possibility to look at practically any relevant close distance. For this reason, the transition region makes the difference to other optical approaches. The understanding of the optical properties of this part is supported by the simple analytical model introduced here.

ACKNOWLEDGMENTS

R. Blendowske acknowledges the support by the Forschungsgemeinschaft Deutsche Augenoptik. This research was supported in part by Ministerio de Educacion y Ciencia, Spain (grant FIS2004-02153).

Received December 28, 2005; accepted March 14, 2006.

REFERENCES

1. Bourdoncle B, Chauveau JP, Mercier JL. Traps in displaying optical performances of a progressive-addition lens. Appl Optics 1992;31: 3586–93.
2. Alvarez LW. Two-element variable-power spherical lens. US Patent 3,305,294. February 21, 1967.
3. Kanolt CW. Multifocal ophthalmic lenses. US Patent 2,878,721. March 1959.
4. Plummer WT. Azygous ophthalmic lens and spectacles for correcting presbyopia. US Patent 3,797,922. March 19, 1974.
5. Sheedy JE, Campbell C, King-Smith E, Hayes JR. Progressive powered lenses: the Minkwitz theorem. Optom Vis Sci 2005;82:916– 22.
6. Villegas EA, Artal P. Spatially resolved wavefront aberrations of oph-

thalmic progressive-power lenses in normal viewing conditions. Optom Vis Sci 2003;80:106–14.
7. Villegas EA, Artal P. Comparison of aberrations in different types of progressive power lenses. Ophthal Physiol Opt 2004; 24:419–26.
8. Villegas EA, Gonzalez C, Bourdoncle B, Bonnin T, Artal P. Correlation between optical and psychophysical parameters as a function of defocus. Optom Vis Sci 2002;79:60–7.
9. Villegas EA, Artal P. Impact of the aberrations of progressive power lenses on visual acuity. Invest Ophthalmol Vis Sci 2003;44:E-abstract 4190.
10. Minkwitz G. [On the surface astigmatism of a fixed symmetrical aspheric surface.] Opt Acta (Lond) 1963;10:223–7.
11. Mahajan VN. Strehl ratio for primary aberrations: some analytical results for circular and annular pupils. J Opt Soc Am (A) 1982;72: 1258–66.

Ralf Blendowske
Fachhochschule Darmstadt
Fachbereich Mathematik und Naturwissenschaften
Optotechnik und Bildverarbeitung
Schöfferstrasse 3, D-64295 Darmstadt, Germany
e-mail: blendowske@fh-darmstadt.de